Use of Support Vector Machines for Classification of Defects in the Induction Motor

Samia BENZAHIOUL[1], Abderrezak METATLA[1], Adlen KERBOUA[1],
Dimitri LEFEBVRE[2], Riad BENDIB[1]

[1] Department of Mechanical Engineering, Faculty of Technology, University of August, 20, 1955,
Skikda, Algeria, e-mail: {s.benzahioul, a.metatla, a.kerboua, r.bendib}@univ-skikda.dz
[2] Department of Electrical Engineering, Faculty of Sciences and Technologies,
University of Le Havre, France, e-mail: dimitri.lefebvre@univ-lehavre.fr

Abstract: The classification and detection of defects play an important role in different disciplines. Research is oriented towards the development of approaches for the early detection and classification of defects in electrical drive systems. This paper, proposes a new approach for the classification of induction motor defects based on image processing and pattern recognition. The proposed defect classification approach was carried out in four distinct stages. In the first step, the stator currents were represented in the 3D space and projected onto the 2D space. In the second step, the projections obtained were transformed into images. In the third step, extraction of features whereas the Histogram of Oriented Gradient (HOG) is used to construct a descriptor based on several sizes of cells. In the fourth step, a method of classifying the induction motor defects based on the Support Vector Machine (SVM) was applied. The evaluation results of the developed approach show the efficiency and the precision of classification of the proposed approach.

Keywords: Induction motor, defect, pattern recognition, SVM, HOG, classification, detection.

1. Introduction

Today, squirrel cage asynchronous machines play an important role in the industrial world not only for their relatively low manufacturing cost, but also for their minimum maintenance requirements and their robustness. The asynchronous or induction machines have several advantages over other types of electrical machines. However, this kind of machines can suffer from some anomalies [1], resulting in the majority of cases in operational constraints that can cause the reduction of both production and yields rates, and in some cases the

process shutdown. Sophisticated supervision systems should be implemented to ensure the continuity and accuracy of operation, the safety of persons, the quality of services and to ensure that decisions are taken on ad-hoc basis. During the last 3 years, considerable efforts have been devoted to the detection and diagnosis of defects in the induction motors, and several researches and methods have been presented. These scientific works may be classified into two main fields.

- Methods based on models
- Methods based on signal processing

The methods of the first type use a reference model which is based on the analytical representation of the induction motor. For example, the method presented in [2] characterizes the winding function using the space harmonics while Tushar et al. [3], proposed a diagnosis method based on the use of direct and quadrature rotor currents to detect winding defects and to distinguish between stator winding defects and unbalanced supply voltage. In [4] authors presented another detection approach based on a multi-winding model. These studies have greatly enriched the modelling oriented points of view towards the diagnosis of defects in the induction motors.

On the other hand, in case of the method based on signal processing, the results are achieved by the extraction and quantification of measurable electrical or mechanical quantities related to defects. Several works have been developed in this context by researching internal and external indicators. Among them we mention the study carried out by Bonnet et al. [5] in the context of diagnosis of various rolling defects in the induction motor. Diallo et al. [6], presented a new method by using pattern recognition to detect rotor and stator defects in induction motors. Decision procedures, based on the k-nearest neighbor rule and direct limit calculation, were used to detect defects. In [7], the author has developed a method for pattern recognition based on a Multi-Layer Perception Artificial Neural Network (MLPANN) in order to detect and identify eccentricity defects and demagnetization of the synchronous machine. In a study presented in [8], the author used an approach that is based on the classical spectral analysis and a method of classification, inspired by the supervised learning theory of support vector machines (SVM), enabling the detection and identification of the ball bearing defect in the induction motor. In [9], the author proposes a technique of diagnosis of rotor electrical defects in the induction motor based on the analysis of acoustic signals collected from three motors.

In this study, we develop a new approach for detection and classification of defects in induction motors using learning algorithms for pattern recognition. The approach permits the detection of defects and classifies the majority of defects accurately and in real time. In order to allow an early classification of defects using the reduction of the number of samples, which facilitates online detection, the approach was optimized. Our goal is to synthesize a new diagnosis approach

and establish criteria of choice for their use in order to make a very advanced practical contribution to the diagnosis of defects in the induction motor. Our contribution can be summarized as follows.

In the literature, many of the works use stator current processing with different signal processing approaches. In our study, instead of using stator current signal, we propose a Machine Learning approach based on image processing to classify defects in the induction motor.

We propose a defect diagnosis approach based on efficient classifier trained on small dataset.

This paper is organized as follows. In the sections 2 and 3 the test bench used in this work is presented. The fourth section concerns a flowchart description of the proposed method. Firstly, the stator currents are presented in the 3D and 2D spaces, followed by an application of two preprocessing operations (normalization and pixelization). Finally, the section was concluded by extracting points of interest and constructing a descriptor HOG. The fifth section is devoted to the presentation of SVM classifier used for classification of defects. The last section contains an experimental phase and discussion of the results. The study has been terminated by conclusion and perspective.

2. Defects in induction motors

A defect of an induction motor means any accidental change in the normal operation. Defects have different origins: electrical, mechanical and magnetic. Statistical studies carried out by [6] on low and medium power induction motors are shown in *Fig. 1*.
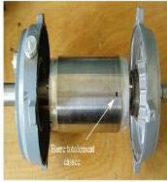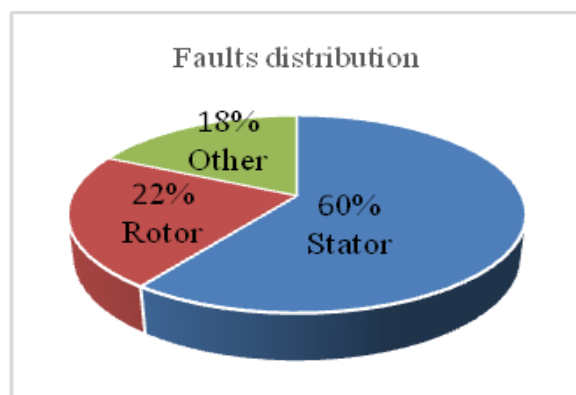

Figure 1: Breakdown of defects in low and medium power induction motors.

In our study, we were interested in presenting at least one defect of each class in order to evaluate its influence on the behavior of the studied induction motor (*Table1*).

Table 1: Description of the defects in induction motors

Defects	Illustration	Causes	Effects
Rolling defect		The rolling defect is generally related to the wear of the bearing and more specifically a degradation of the balls, *Wear due to aging, *High operating temperature, *Loss of lubrication, *Contaminated oil.	Oscillation of the load torque, *Appearance of additional losses, *Vibration by the displacement of the rotor around the longitudinal axis, *Generates impact on the power supply.
Broken bar defect		The break can be located either at its notch or at the end which connects to the rotor rings *The breaking of rotor bar is generally caused by: rotor/stator friction.	Induction of stator current harmonics in the winding *Reduction of the average value of the electromagnetic torque, *Increased oscillations of the rotation speed, *Mechanical vibration, abnormal operation of the machine
Short circuit fault		A short circuit defect for the same phase originates from an isolation defect in the concerned winding	An increase of the stator current in the affected phase, with a slight variation of the amplitude on the others, *Modification of the power factor and increase of the rotor circuit currents, *Increased temperature of the winding and accelerated isolation degradation.

Different operation modes of the induction motor chosen for this study are listed in *Table 2* [10].

In the remainder of this paper, the following notations are used to denote different operating scenarios of the induction motor:

* Normal operating state: *h,*
* Rolling defect: f_1,
* Broken rotor bar: f_2,
* Short circuit defect 2% (f_3),
* Short circuit defect 5%.

Table 2: Operation modes of the induction motor used

Motor operating state	The loads %	Number of tests
Normal operating state (*h*)	20,50, 100	60
Rolling defect (*f₁*)	0, 20, 60, 100	22
Broken rotor bar defect (*f₂*)	0, 20, 60, 100	80
Short circuit defect 2% (*f₃*) (Short circuit 2% means that 2% of the total number of turns are short circuited)	10, 20, 40	15
Short circuit defect 5% (*f₄*) (Short circuit 5% means that 5% of the total number of turns are short circuited)	10, 20, 40	15
	Total	192

A test bench was realized to perform different scenarios or operating modes of an induction motor 450 W, 127V, 50 Hz, a pole pair and rotational speed 1480rpm.

All the acquisitions were carried out at steady state over a period of 10 seconds, with sampling frequency equal to 10 KHz, i.e. 100001 samples for each of the following measured signals [10]:

* The line current of three stator phases,
* The three supply voltages,
* The electromagnetic torque.

3. The proposed approach used for defect detection

The principle of the approach developed in this work is based on the use of pattern recognition techniques in images representing the characteristic signals of each operation mode.

Our approach is divided into four stages. In the first step, we represent the magnitudes of the three phase system of the stator currents in the 3D space, followed by a projection on the three 2D spaces. In the next step, the preprocessing operations were performed. Firstly, scaling of the heterogeneous data was performed to facilitate their comparison. Secondly, a pixelization operation of the data was performed (graphical representation for the signals in 2D space). In the third step, a descriptor was computed by HOG algorithm containing a set of points of interest represented by two essential parameters, which are the modulus and the orientation of the local gradient [11]. In the last step, SVM classifier was used to label different operating scenarios of the induction motor [12]. The different stages of the developed approach are presented in *Fig. 2*.
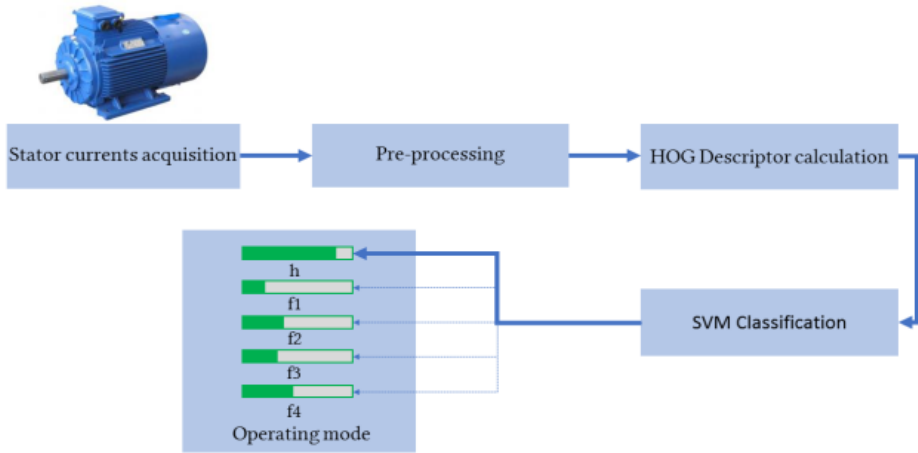

Figure 2: Architecture of the used classification methodology.

4. Representation of the currents in 3D space and the projection of the trajectories in 2D spaces

In general, a system of three quantities of the same nature and frequency is the superposition of three balanced systems of the same frequency: a three-phase direct system, a three-phase inverse system and a homopolar system. In practice, this means that the system of the three voltages or of the three currents can be represented by the components x_d, x_i and x_0 (voltages or currents) such that [10]:

x_d: represents the direct symmetrical component,
x_i: represents the inverse symmetrical component,
x_0: represents the homopolar component.

The 3D graphical representation of the three-phase stator currents also makes it possible to present plans or surfaces defined by a parametric equation or by a Cartesian equation of type:

$$z = f(x,y) \tag{1}$$

with $x = c$, $y = i_{bs}$ and $z = i_{cs}$.

The projection of the three stator currents is in the parallel type projection plane depending on whether the projection direction is perpendicular to the projection plane xoy, xoz and yoz.

In the case of the three-phase currents in healthy induction motor, the projections of currents $i_{as} = f(i_{bs})$, $i_{cs} = f(i_{as})$ and $i_{bs} = f(i_{cs})$ on the three planes xoy, xoz and yoz, are called Lissajous curves. This presentation has a circular shape centered at the origin and diameter equal to the magnitude of the stator currents corresponding to the state of operation of the machine. In the case of the faulty motor, the Lissajous curve changes in shape and thickness due to the presence of the harmonics created by the fault. This strategy consists in comparing the curves of Lissajous that result from the operation with and without faults. This strategy is not valid in our case because of the use of a real database containing measurement noise and state which makes lose the centered form of the Lissajous curve. For this purpose, we proposed a technique based on the transformation of the Lissajous curve into an image, then we applied the SVM for the detection and classification of defects.
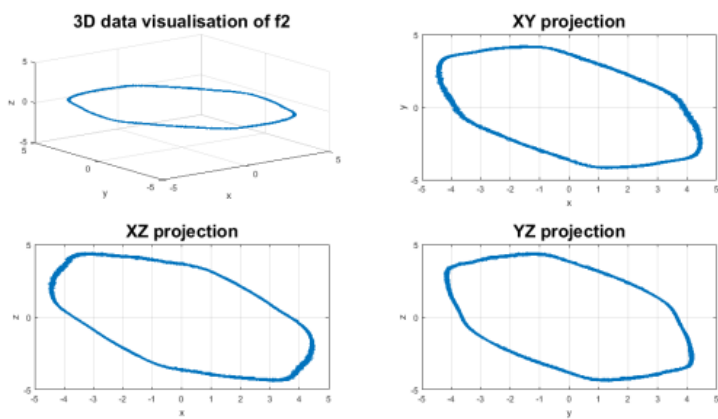
Fig. 3 shows in different operation modes the three phase stator currents i_a, i_b and i_c in the 3D space, and the projections of the trajectories in 2D space by applying (1). It was found that each mode of operation corresponds to a specific shape of the projections.

(a)

(b)

(c)
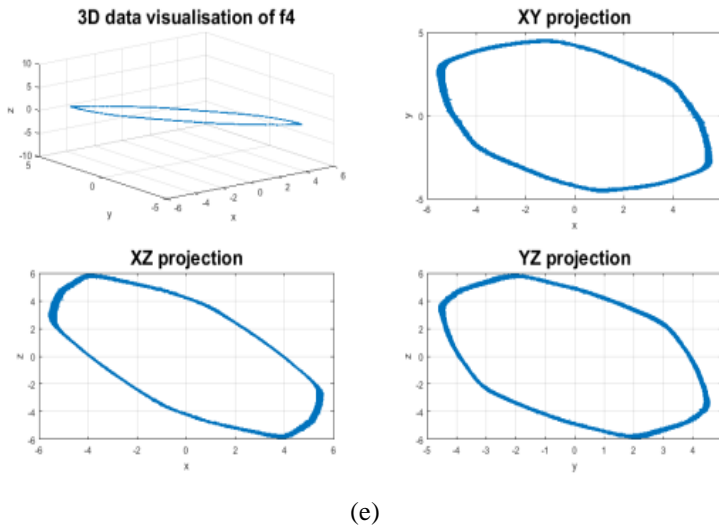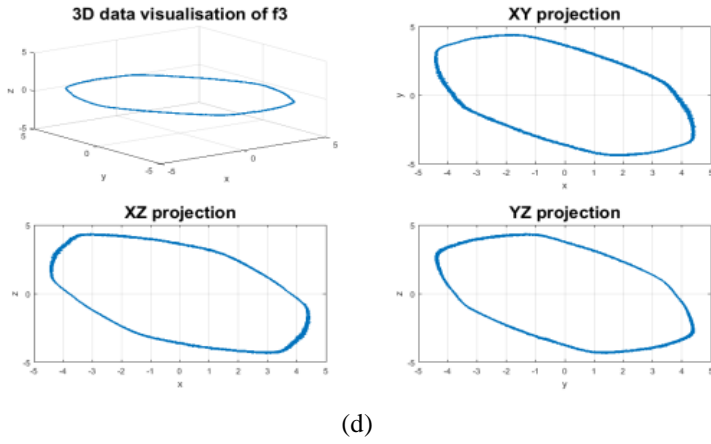
(d)

(e)
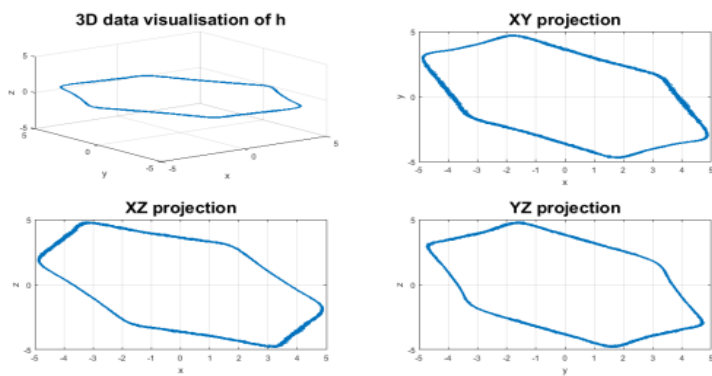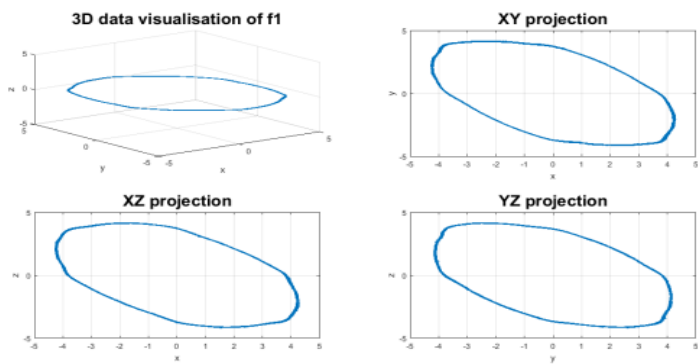
Figure 3: Representation of three stator currents in 3D space and projection in 2D planes for each operation mode*: a.* Healthy state; *b.* Rolling fault; *c.* Bearing fault; *d.* Short circuit fault 2%; *e.* Short circuit fault 5%.

5. Preprocessing

This step involves two operations. Firstly, normalization of the data (standardization) was carried out to a range [-1, 1] and, secondly, a pixelization step [13] is applied.

5.1. Normalization step

In order to compare the different magnitudes and to minimize the interclass variations with respect to the applied load, the scaling is done to let the data belong to [-1, 1]. *Fig. 3* illustrates the stator current with different loads before and after normalization. It can be seen that the change in load affects the shape size. For 20 % load (*Fig. 4.a*), signals vary in the range [-5, 5], while a 100% load generates oscillating signals in a range [-9, 9]. The shapes represent the same operating state (interclass variation), which can lead to confusion for the classifier. After standardization (*Fig. 4.b*), the set of signals is included in the same interval [-1, 1].

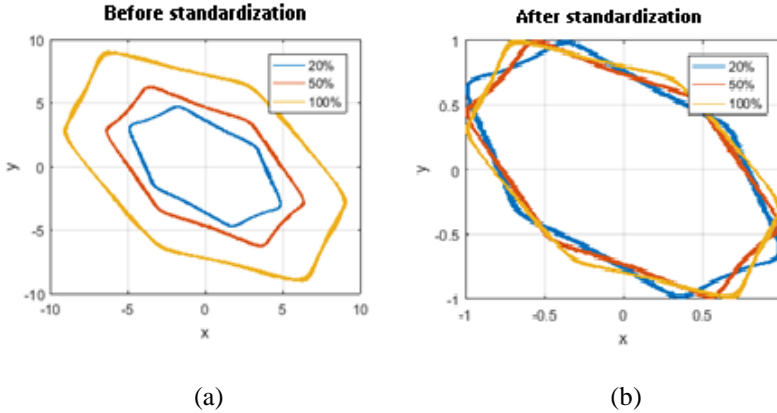
(a)   (b)

Figure 4: *a.* Before standardization; *b.* After standardization

The applied algorithm is expressed by the following formula by posing: [lim_1, lim_2] = [-1, 1].

We can write:

$$\begin{cases} i_a = (\dfrac{i_a - \min(i_a)}{\max(i_a) - \min(i_a)} * (\lim_2 - \lim_1)) + \lim_1 \\[3mm] i_b = (\dfrac{i_b - \min(i_b)}{\max(i_b) - \min(i_b)} * (\lim_2 - \lim_1)) + \lim_1 \\[3mm] i_c = (\dfrac{i_c - \min(i_c)}{\max(i_a) - \min(i_c)} * (\lim_2 - \lim_1)) + \lim_1 \end{cases} \qquad (2)$$

This operation results in keeping all characteristics of the appearance of the pattern.

5.2. Pixelization step

It is the transformation of the 2D data to a graphic from (image) by the representation of each signal sample measured by a pixel of intensity corresponding to the value of the reduced dimension so as not to lose the information relative to it:

For example, a pixel in the XY plane is represented by its coordinates (x,y) corresponding respectively to the two currents i_a and i_b, while the pixel intensity is the value of i_c. In fact, each measured signal sample was represented by the coordinates and the gray level intensity of one pixel to produce specific pattern for every operating mode. The algorithm applied for the three planes XY, YZ and XZ is as follows:

$$\begin{cases} (i_a * resolution, \, i_b * resolution) = i_c \\ (i_c * resolution, \, i_a * resolution) = i_b \\ (i_b * resolution, \, i_c * resolution) = i_a \end{cases} \qquad (3)$$

Given that i_a, i_b and $i_c \in [-1, 1]$, these transformations allows us to obtain positive and not null integer indices which can be positioned in 2D images with well-defined resolutions. Our algorithm is based on the processing of images faithfully representing the system evolution in relation to time while being of reduced sizes in order to speed up the training process. In our case several resolutions have been used such as (64*64), (128*128), (256*256) and (512*512). The following figure illustrates the obtained images.
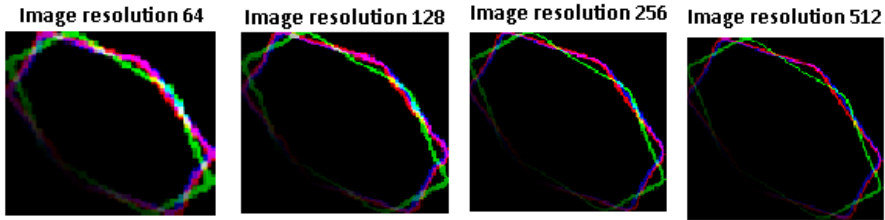
Figure 5: Image with different resolutions.

It can be that the image resolution (128*128) represents almost the same level of detail as the image resolution (256*256) while having only a quarter of pixel (1/4). However, the image resolution (128*128) loses fine detail. So our choice is to use the image resolution (256*256) which represents a good compromise between the data size of the encoded image and the level of desired detail.

6. Construction of the descriptor

Local characteristics refer to pattern or structure distinct immediate surroundings by texture, color or intensity. Their descriptors which are compact vector representations of a local neighborhood are the constitutive elements of many algorithms of computer vision. Their applications include pattern recognition, image recording, object detection and classification [14].

In our algorithm, we used the descriptor HOG adapted to the tasks of classification of deformable objects. It decomposes the image into square cells of a given size (CellSize) covering the entire image on one hand, and it computes, on the other hand, a histogram of oriented gradients in each cell by constructing the image gradient $\nabla \ell$ (x, y) and using the central difference [11].

The images obtained during the pixelization phase have particular shapes for each mode of operation of the induction motor. This change of shape from one state to another, once characterized in a robust manner by the extraction of a HOG descriptor, can be used to train the classifier. Therefore, it is important to make sure that the HOG feature vector encodes the right amount of information about the local orientations in the images. The effect of the cell size parameter on the amount of the shape information encoded in the feature vector can be seen by varying the HOG cell size parameter ([4 4], [8 8], [16 16], [32 32] and [64 64]) and visualizing the result presented in *Fig. 6*.
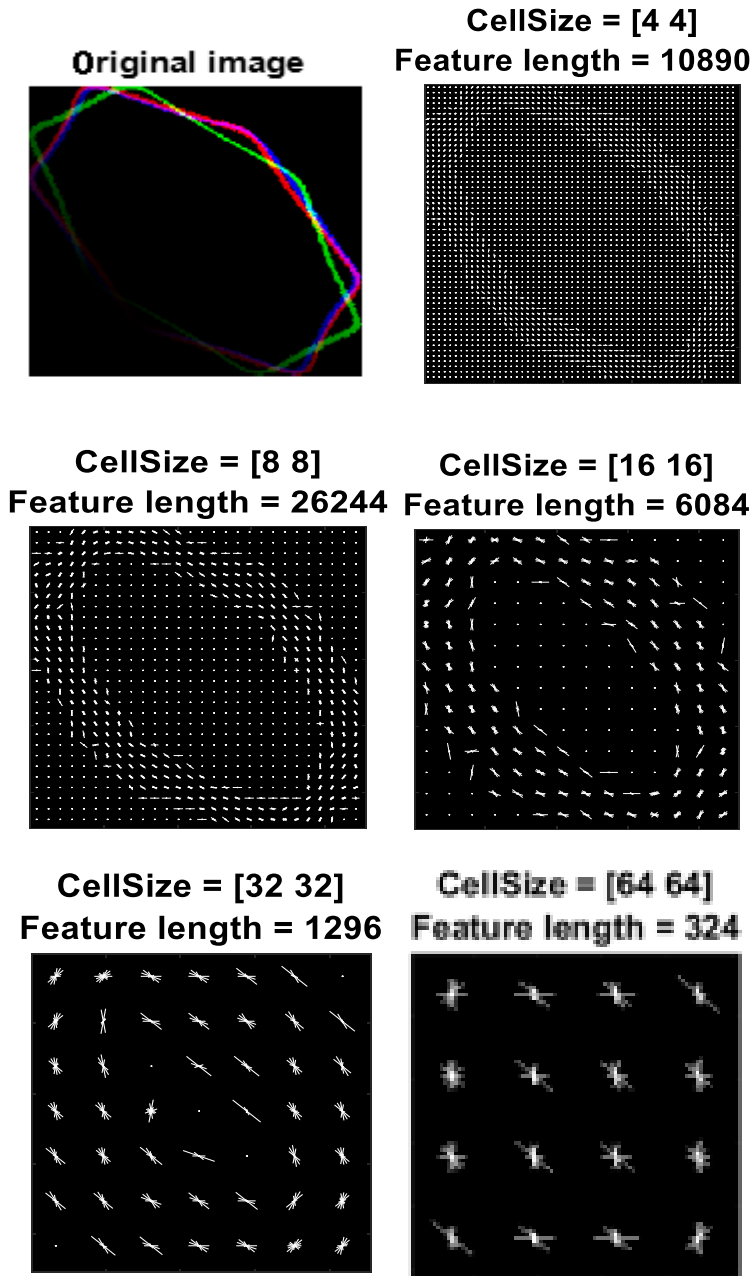
Figure 6: Effect of the cell size on the HOG descriptor.

It is found that cell sizes [64 64] and [32 32] do not give sufficient information about shapes, whereas a cell size of [4 4] contains a lot of shape information, but increases substantially the descriptor size. A good compromise would be to choose the two intermediate cell sizes [8 8] and [16 16] which are evaluated during the experimentation phase. This adjustment of the chosen cell size has sufficient information to enable us to visually differentiate the shape corresponding to the operating state concerned, while limiting the size of the descriptor, which makes it possible to accelerate the driving phase.

We assume that the final descriptor is the concatenation of the three descriptors extracted from the three images of the 2D projections (XY, YZ and XZ) as follows:

$$HOG = \left[HOG_{x,y}, \; HOG_{y,z} \;, \; HOG_{x,z} \right] \tag{4}$$

Using the cell size of [8 8] for each of the three-projection images, a total number of 34596*3=103788 points of interest have been obtained. For the first descriptor [16 16] we get 8100*3=24300 points of interest.

Since the obtained descriptor contains noise and redundant information, which affect the classification score and lead to unnecessary increases in the computation time. The application of the Principal Component Analysis (PCA) algorithm eliminates redundancy and noise. It is found that the 573 most representative elements contain more than 98% of the distinctive information.

7. Support vector machines (SVM) and mathematical principle

Support Vector Machines (SVM) are a set of supervised classification techniques. SVMs were developed by Vapnik et al. [15] as part of a statistical theory of learning. The SVMs have been applied to many fields and have become one of the most widely used models for classification and regression. The basic use of SVMs is the resolution of binary problems with two classes.

An SVM algorithm classifies the data by calculating the best hyper-plane that separates all the points belonging to one class from those of the other class. The best hyper-plane is the one with the widest margin between the two classes. The SVM is represented by the data points closest to the separation hyper-plane and those at the edge of the class to which the closest class belongs. *Fig. 7* illustrates this definition [16].
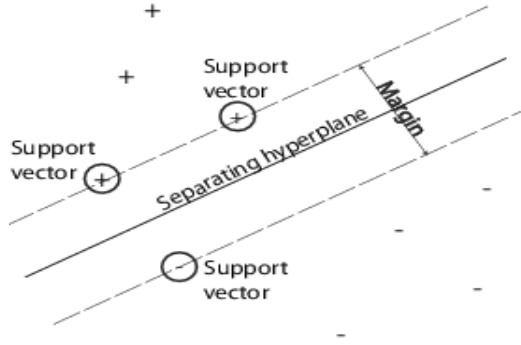
Figure 7: Principle of the SVM.

The + indicates the points of the first class, the − indicate the points of the second class.

The training data are a set of points or vectors x_i with their categories y_i. For some dimension d the $x_j \in R^d$, and the $y_j = \pm 1$. The equal of the hyper-plane is given by:

$$f(x) = x^T \beta + b \tag{5}$$

where, $\beta \in R^d$ and b are real numbers.

The next problem defines the best separation hyper-plane between the two classes (i.e. the decision boundary). The calculation of β and b serves to minimize $\|\beta\|$ such that for all the vectors (x_j, y_j).

$$y_j f(x) \geq 1 \tag{6}$$

The support vector machines values x_i on the boundary between the two classes which satisfy the following condition:

$$y_j f(x) = 1 \tag{8}$$

The problem can be seen as a minimization of $\|\beta\|$ which is a quadratic programming problem. The optimal solution (β, b) makes it possible to classify a vector z according to the following formalization:

$$class(z) = sign(z^{'}\hat{\beta} + b) = sign(\hat{f}(z)) \tag{9}$$

where $\hat{f}(z)$ is the classification score which represents the distance of the vector z with respect to the decision boundary.

SVMs were originally developed to handle binary problems but they can be adapted for the handling of multi-class problems. We can distinguish two main

schemes: the first "one against all", which consists in transforming the problem with k classes into k binary classifiers, whereas the second one is called "one against one", this strategy consists in transforming into (k*(k-1))/2 binary classifiers. In this work,we focus on the supervised classification of defects in the induction motor by the use of an OVA (One Versus All) multi class SVM [12,14].

This type reduces the classification problem with three or more classes into a set of simple binary classifiers. For each binary classifier, one class is positive and the others are considered negative. The chosen scheme requires a coding model which determines the training classes and a coding scheme which determines the aggregation of the prediction of the binary classifiers.

In this work, we have five (05) classes (h, f_1, f_2, f_3 and f_4) and consequently five classifiers. The coding model is represented by the coding matrix M of 5 rows and 5 columns. Each row represents a class and each column represents the SVM responsible for detecting the corresponding class as indicated in *Table 3*.

Table 3: Coding model or coding matrix M

Class \ SVMs	SVM$_1$	SVM$_2$	SVM$_3$	SVM$_4$	SVM$_5$
h	+	-	-	-	-
f_1	-	+	-	-	-
f_2	-	-	+	-	-
f_3	-	-	-	+	-
f_4	-	-	-	-	+

For the cells containing "+" the classifier should group all the observation in the classes corresponding to the positive class.

On the other hand, for the cells containing "−"the observation should be grouped in the classes corresponding to the negative class.

If m_k is the element of the matrix M at the row k and the column i ($k, i \in \{1,2,3,4\}$), and s is the score of the classification of the positive class of the classifier SVM$_1$, then a new observation is assigned to the class (k) which minimizes the aggregation of the losses for the SVM$_1$ according to equations (9)

$$\hat{k} = (\mathrm{argmin}_k \left(\sum_{i=1}^{5} |m_{ki}| g(m_{ki}, s_i)) / \sum_{i=1}^{5} |m_{k,i}| \right) \tag{9}$$

8. Experiments

To be able to diagnose defects quickly, there is a need to make compromise between training speed, memory usage, accuracy and interoperability. This is

why we have chosen to use in this work a multi-class SVM classifier of the OVA type, with a cubic function of the kernel without standardization of the data that has already been done during the preprocessing phase.

Our algorithm is essentially written in MATLAB. We used Image Processing Toolbox TM and Statistics and Machine Learning Toolbox TM. The application is run on a Core i3 processor with a clock of 2.4GHz and 6GB of RAM.

The experiment consists of several scenarios starting with an evaluation of the distinctive strength of our descriptor. In order to make an equitable evaluation of the performance of our method, the Cross-validation protocol with K-Folds (K is equal to five), we partition the data into five (5) randomly chosen subsets. Each subset is used to validate the classifier driven on the rest of the subset. This process is repeated K times (K=5 in our case) so that each subset is used exactly once for validation. The mean of the cross-validation error is used as a performance indicator in order to avoid the phenomenon of over-fitting.

As the classification score obtained by classifying them with descriptors obtained using cells of sizes [8 8] and [16 16] is the same, *Fig.8* illustrates the confusion matrices obtained by the SVM classifier with a descriptor using cells of sizes [8 8].
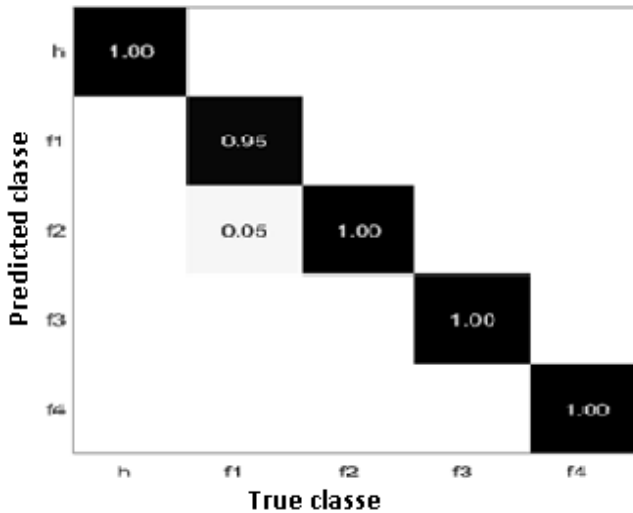

Figure 8: Confusion matrix obtained by the SVM driven by HOG
using cells of sizes [8 8].

It is found that the results obtained by the SVM classifier driven by HOG descriptors using cells of sizes [8 8] and [16 16] give the same overall classification score of 99.5%. In both cases, only one operating state was misclassified, i.e. an operating state with a fault f_1 was mistakenly classified as a defect in f_2 with a percent of 5%. The use of a descriptor with cells of size [16 16] gives a faster execution response than that of the descriptor with cells of size [8 8], with an execution time of 1.8077 and 6.2389 seconds respectively.

9. Accuracy of defect classification

To ensure the safety of people and equipment in industrial field a system is needed to know the occurrence of a defect in real time. These type of systems are affected by two main factors:
1. The time needed to make a good prediction,
2. The time needed to make a good decision.
We test our method by reducing the number of samples necessary to create a descriptor to obtain a good classification (minimization of execution time or fast response speed), in order to evaluate the minimum number of samples necessary to obtain a good classification of the defects. *Fig. 9* illustrates the number of samples necessary to give a good decision with the classifier used.
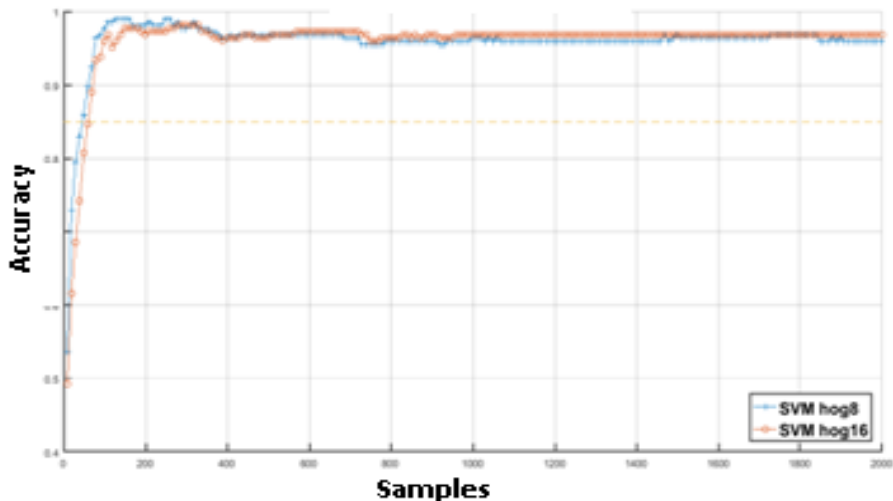

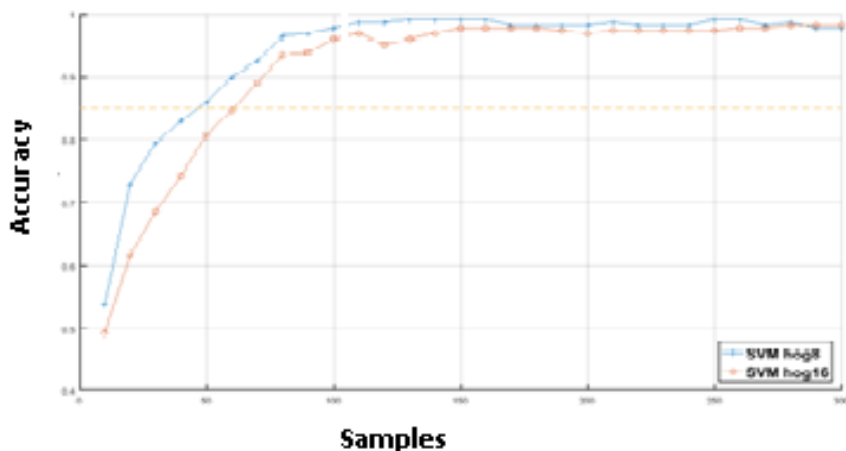*Figure 9*: Minimum number of samples for decision.

Figure 10: Minimum number of samples for decision.

As illustrated in *Fig.10*, it can be seen that the use of 10% to 15% of the samples is sufficient to achieve a score equivalent to the best score obtained in the previous experiment and using all the data.

10. Conclusion

This paper has focused on classification of induction motor defects, especially on the stator short circuit, the broken rotor bar and the rolling defect.

Through this work, it was shown that the monitoring and diagnosis of defects in the induction motor by stator current monitoring is an essential tool for obtaining clues as to the operating state of the induction motor. The occurrence of a defect causes a change in the shape and position of the stator currents represented in the 3D or 2D plane. The use of the pattern recognition technique makes it possible to detect and even identify certain defects in the induction motor, but the use of this technique remains limited for classification and quantification of defects. To this end, a new approach has been proposed for monitoring and classifying these defects. The proposed approach is developed through the realization of several steps starting by representing the stator currents in 3D space and the projection of their trajectories in 2D space followed by the pixelization process where the image resolution 256*256 represents a good compromise. The last step is dedicated to the construction of the descriptors with different sizes of the cells. The results obtained by the various descriptors show that the descriptors using cells of sizes [8 8] and [16 16] present a good compromise and have sufficient significant information. The results obtained also

show that the developed approach gives a good classification score of the majority of defects with good decision and fast response. In our future work, an attempt will be made to develop modern techniques, classify defects with good accuracy and to increase response speed in more complicated systems such as multi-source energy systems.

References

[1]   Ondel, O., Boutleux, E., and Clerc, G., "A method to detect broken bars in induction machine using pattern recognition techniques", *IEEE Transactions on Energy Conversion, Institute of electrical and Electronics engineers*, vol 20 (3), 2006, pp. 512-519.

[2]   Toliyat, H. A., and Lipo, T. A., "Analysis of a concentrated winding induction machine for adjustable speed drive applications. Part 2: Experimental results", *IEEE Transaction on Energy Conversion*, vol. 9(4), 1994, pp. 695-700.

[3]   Vilhekar, T. G., Ballal, S. M., and Suryawanshi, H. M., "Detection of winding faults in wound rotor induction motor using loci direct and quadrature axes of rotor currents", *Electrical power components and systems*, vol. 45, (11), 2017, pp 1217-1230.

[4]   Ritchie, E., Deng, X., and Jokinen, T., "Dynamic model of 3-phase squirrel cage induction motors with rotor faults", *ICEM '94*, B6(2), France, 2004, pp. 694-698.

[5]   Bonnett, A. H., "Cause and analysis of anti-friction bearing failures in A.C induction motors", *IEEE Transactions on Industry Application*, *Sept/Oct*, 1993, pp. 14-23.

[6]   Diallo, D., Benbouzid, M. E., Hamad, D., and Pierre, X., "Fault detection and diagnosis an induction machine Drive: A pattern recognition approach based on Concordia stator mean current vector", *IEEE Transactions on energy conversion, Institute of electrical and Electronics engineering*, vol 20 (3), 2005, pp 512-519.

[7]   Guota, K., and Kaut, A., "A review on fault diagnosis on induction motor using artificial neural networks", *International journal of science and research*, Vol, 3(7). pp. 680-684, 2014.

[8]   Tafinine, F., Mokrani, F., Antoni, K., Kabla, J., and Asradj, Z., "Introduction des SVM en MCSA", *4th International conference, Sciences of electronic, technologies of information and telecommunications*, pp.1-7 *March 25-29, Tunisia*, 2007.

[9]   Glowacz, A., "Recognition of acoustic signals on induction motors with the use of MSAF10 and bayes classifier", *Arc. Metall. Mater*, vol, 60 (1), 2016, pp. 153-158.

[10] Sahraoui, M., Ghoggal, A., Zouzou, S., and Benbouzid, E. M. E., "Dynamic eccentricity in squirrel cage induction motors-simulation and analytical study of its spectral signatures on stator currents", *Simulation Modelling Practice and Theory*, 2008, pp. 1503-1513.

[11] Navneet, D., and Triggs, B., "Histograms of oriented gradients for human detection", *International Conference on computer Vision and Pattern recognition, (CVPR'05)*, *San Diego, United States*, pp.886-893, 10.1109/CVPR.2005.177. inria-00548512.

[12] Christianini, N., and Shawe-Taylor, J., "An Introduction to Support Vector Machines and Other Kernel-Based Learning Methods", computer science, mathematics, *Cambridge University Press*, *Cambridge, UK,* pp. 103-109. Published 2000. DOI: 10.1017/CBO9780511801389.012

[13] Hadef, M., Djerdir, A., Ikhlef N., Mekideche, M. R., and N'diaye, A. O., "A Fault severity index for stator winding faults detection in vector controlled PM synchronous motor", *J. Electr Eng Techno*, vol 10 (6), pp.2326-2333 2015.

[14] Namdarin, M., and Jazayeri-Rad, H., "Incipient fault diagnosis using support vector machines based on monitoring continuous decision functions", *Engineering Applications of Artificial Intelligence*, vol 28, 2014, pp 22-35.

[15] Weston, J., and Watkings, C., "Support vector machines for multi-class pattern recognition", In *Proceedings of the Seventh European Symposium on Artificial Neural Networks* (*ESANN 1999*), pp. 219-224. MIT Press, Combridge, MA,1999.

[16] Vapnik, V., "Statistical Learning Theory", *Wiley, New York,* 1998.

[17] Gelbart, M., Snoek, J. R., and Adams, P., "Bayesian Optimization with Unknown Constraints", *http://arxiv.org/abs/1403.5607*, 2014.